Correlated photoionization processes in H⁻

M. S. Pindzola and F. Robicheaux

Department of Physics, Auburn University, Auburn, Alabama 36849

Correlated photoionization processes in H⁻ are calculated by a numerical solution of the time-dependent Schrödinger equation on a partitioned lattice. Projection of the time evolved wave function onto lattice eigenstates for H yields cross sections for photoionization with excitation and double photoionization. The lattice results confirm the surprisingly large double to single photoionization ratios for H⁻ found in the recent *R*-matrix calculations of Meyer, Greene, and Esry, Phys. Rev. Lett. **78**, 4902 (1997).
[S1050-2947(98)08411-X]

PACS number(s): 32.80.Fb

Recently, various correlated photoionization processes in helium were calculated by direct solution of the time-dependent Schrödinger equation [1]. Cross sections for simultaneous photoexcitation and photoionization, as well as double photoionization, were calculated by the time propagation of a coupled set of two-dimensional partial differential equations on a numerical lattice. This method utilized distributed memory parallel computers by partitioning the two-dimensional radial wave function over many processors. The calculated cross sections for helium were found to be in excellent agreement with recent benchmark experiments carried out at synchrotron light source facilities [2–4]. At present photoionization experiments on two-electron atomic ions are only in the planning stages. As a guide to future experiments and for comparison with existing theoretical predictions [5–7], we present in this Brief Report further lattice solutions of the time-dependent Schrödinger equation for correlated photoionization processes in the negative hydrogen ion.

The ground state of H⁻ is found by relaxation of the time-dependent Schrödinger equation in imaginary time ($\tau = it$):

$$-\frac{\partial \phi_0(\vec{r_1},\vec{r_2},\tau)}{\partial \tau} = H_{\text{atom}}\phi_0(\vec{r_1},\vec{r_2},\tau), \quad (1)$$

where H_{atom} is the nonrelativistic Hamiltonian for the three-body system with the nucleus at the origin of the coordinate system. The expansion for the ground-state wave function of H⁻ is given by

$$\phi_0(\vec{r_1},\vec{r_2},\tau) = \frac{1}{r_1 r_2}[P_{ss}^{1S}(r_1,r_2,\tau)Y_{ss}^{S} + P_{pp}^{1S}(r_1,r_2,\tau)Y_{pp}^{S}$$

$$+ P_{dd}^{1S}(r_1,r_2,\tau)Y_{dd}^{S}], \quad (2)$$

where $P_{\ell_1,\ell_2}^{LS}(r_1,r_2,\tau)$ are two-dimensional reduced radial wave functions and Y_{ℓ_1,ℓ_2}^{L} are coupled spherical harmonics in the remaining angular coordinates. Upon substitution of Eq. (2) into Eq. (1), the angular coordinates are integrated out to yield three coupled partial differential equations for the three reduced radial wave functions. The coupled time-dependent equations are solved on a two-dimensional lattice

using an explicit time propagator. Initially, $P_{ss}^{1S}(r_1,r_2,\tau=0)=P_{1s}(r_1)P_{1s}(r_2)$, where $P_{1s}(r)$ is the reduced radial orbital for the ground state of hydrogen, and $P_{pp}^{1S}(r_1,r_2,\tau=0)=P_{dd}^{1S}(r_1,r_2,\tau=0)=0$. Since there are no electron spin operators in H_{atom}, the initial choice of a spatially symmetric wave function is preserved throughout the imaginary time propagation of the Schrödinger equation. Relaxation was carried out using two different lattice spacings, $\Delta r=0.2$ and $\Delta r=0.1$. On the coarse mesh the final energy for the ground state of H⁻ is found to be $E_0=-0.5220$ a.u., while on the fine mesh the energy is $E_0=-0.5260$ a.u. The energy on the fine mesh is within 0.3% of the exact energy of -0.5277 a.u. On the coarse mesh the ionization potential of H⁻ is found to be 0.726 eV, while on the fine mesh it is 0.741 eV. The experimental ionization potential is 0.755 eV. The probability density associated with the $P_{ss}^{1S}(r_1,r_2,\tau=100$ a.u.) radial wave function on the coarse mesh is shown in Fig. 1. The butterfly shape is characteristic of a two-electron system in which one electron is near the nucleus while the other electron extends to much larger dis-
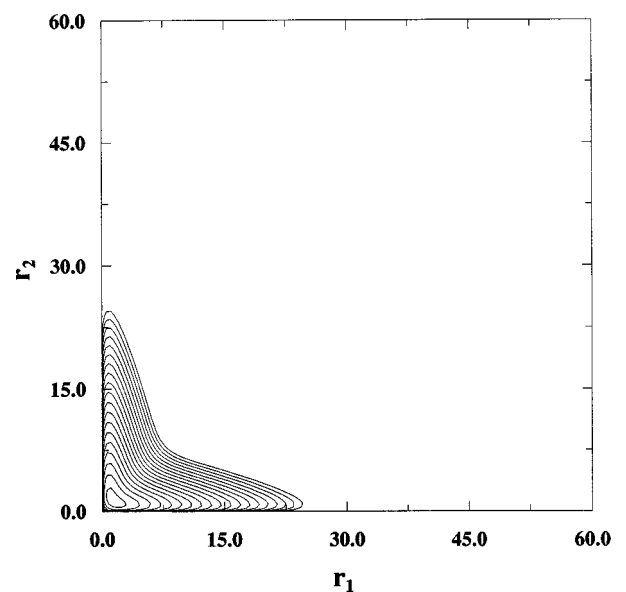

FIG. 1. Probability density associated with the ss ¹S radial wave function of the ground state of H⁻.

TABLE I. Photoionization cross sections and ratios for H⁻ calculated using the time-dependent close-coupling method with a lattice spacing of 0.2 (Mbarn = 1.0×10^{-18} cm²).

Energy (eV)	Single ($n=1$) (Mbarns)	Double (Mbarns)	$\dfrac{\text{Single}(n=2)}{\text{Single}(n=1)}$	$\dfrac{\text{Single}(n=3)}{\text{Single}(n=1)}$	$\dfrac{\text{Double}}{\text{Single }(n=1,2,3)}$
20.0	1.075	0.150	71.4%	9.26%	7.73%
25.0	0.596	0.095	70.2%	7.40%	8.99%
30.0	0.364	0.058	68.7%	6.15%	9.17%
35.0	0.240	0.037	67.5%	5.16%	8.91%
40.0	0.166	0.024	66.5%	4.39%	8.51%
50.0	0.089	0.011	65.7%	3.30%	7.61%

tances. The probability densities associated with the $P_{pp}^{1S}(r_1, r_2, \tau = 100$ a.u.) and $P_{dd}^{1S}(r_1, r_2, \tau = 100$ a.u.) radial wave functions are concentrated much closer to the origin of the coordinate system, since correlation effects are strongest when the electrons are near each other.

With the ground state of H⁻ in hand, we now solve the "weak field" time-dependent Schrödinger equation in real time:

$$i\frac{\partial \psi(\vec{r}_1, \vec{r}_2, t)}{\partial t} = H_{\text{atom}} \psi(\vec{r}_1, \vec{r}_2, t)$$
$$+ H_{\text{rad}} \phi_0(\vec{r}_1, \vec{r}_2, \tau = 100 \text{ a.u.}) e^{-iE_0 t}, \quad (3)$$

where H_{rad} is the Hamiltonian for interaction with a time-dependent radiation field. The second term on the right-hand side acts as a source for the time evolution of $\psi(\vec{r}_1, \vec{r}_2, t)$, which is set to zero at time $t=0$. The full time-dependent Schrödinger equation may be recovered by adding a term $H_{\text{rad}} \psi(\vec{r}_1, \vec{r}_2, t)$ to the right-hand side of Eq. (3). The expansion for the total wave function of H⁻ is given by

$$\psi(\vec{r}_1, \vec{r}_2, t) = \frac{1}{r_1 r_2} [P_{sp}^{1P}(r_1, r_2, t) Y_{sp}^P + P_{pd}^{1P}(r_1, r_2, t) Y_{pd}^P$$
$$+ P_{df}^{1P}(r_1, r_2, t) Y_{df}^P] \quad (4)$$

plus a similar expansion with $\vec{r}_1$ and $\vec{r}_2$ interchanged. Substitution of Eq. (4) into Eq. (3) yields six coupled partial differential equations for the six reduced radial wave functions. After time propagating the coupled equations for 10 optical periods, photoionization probabilities are extracted by projecting the total wave function onto bound lattice eigenstates of the one-electron hydrogen atom. Cross sections for photoionization with excitation and for double photoionization are then calculated from the rate of change of the photoionization probability divided by the photon flux.

We calculated correlated photoionization cross sections for H⁻ at six energies well above the complete photofragmentation threshold of 14.36 eV. Two lattices are employed: one with 300×300 points and $\Delta r = 0.2$ and a second with 600×600 points and $\Delta r = 0.1$. Our cross section results are presented in Tables I and II. There is little change in the cross section values for H⁻ in going from the coarse to the fine mesh, in contrast to the 5% to 10% change found in the same type of cross section values for He [1]. This is due in part to the larger radial extent of the H⁻ ground-state wave function. Also, changing the overall box size of the lattice from $R=60$ had little effect on cross sections and ratios at the chosen photon energies. Besides the check on lattice size and spacing, we carried out further calculations at 20 eV with larger wave-function expansions. Adding a $P_{ff}^{1S}(r_1, r_2, \tau) Y_{ff}^S$ term to Eq. (2) changed the energy E_0 by 0.04%, while adding the terms $P_{fg}^{1P}(r_1, r_2, t Y_{fg}^P$ and its interchange to Eq. (4) changed the cross sections by at most 5%.

The total photoabsorption cross sections for H⁻ reported in Table II are within 10% of the total cross sections reported by Broad and Reinhardt [5] in the energy region above the total fragmentation threshold. The double photoionization cross sections for H⁻ in Table II fall within the length and velocity gauge variational configuration-interaction calculations of Nicolaides et al. [6] for the higher photon energies (35 eV to 50 eV), but are substantially above the length gauge calculations at the lower photon energies (20–30 eV).

TABLE II. Photoionization cross sections and ratios for H⁻ calculated using the time-dependent close-coupling method with a lattice spacing of 0.1 (Mbarn = 1.0×10^{-18} cm²).

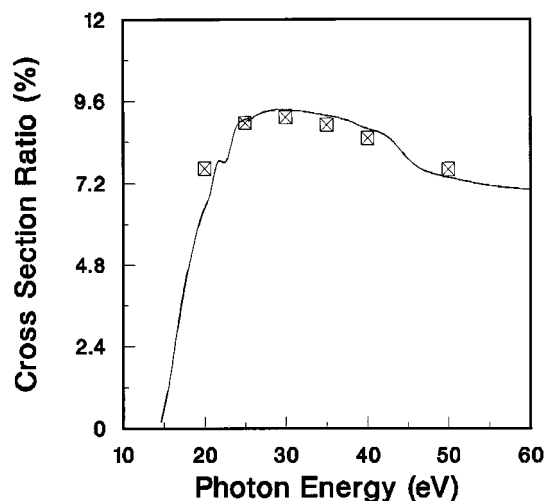| Energy (eV)	Single ($n=1$) (Mbarns)	Double (Mbarns)	$\dfrac{\text{Single}(n=2)}{\text{Single}(n=1)}$	$\dfrac{\text{Single}(n=3)}{\text{Single}(n=1)}$	$\dfrac{\text{Double}}{\text{Single }(n=1,2,3)}$
20.0	1.116	0.152	70.2%	9.11%	7.62%
25.0	0.621	0.098	69.1%	7.27%	8.95%
30.0	0.382	0.061	67.7%	6.03%	9.13%
35.0	0.252	0.038	66.5%	5.05%	8.89%
40.0	0.175	0.025	65.5%	4.30%	8.50%
50.0	0.094	0.012	64.7%	3.21%	7.60%

FIG. 2. Double to single photoionization cross section ratio for H⁻. Crossed box, time-dependent close-coupling method with a lattice spacing of 0.1; solid curve, time-independent R-matrix method [1].

The double to single photoionization cross section ratios for H⁻ in Table II are compared with the recent time-independent R-matrix results of Meyer, Greene, and Esry [7] in Fig. 2. Although the double to single ratios for H⁻ reported by Meyer *et al.* are surprisingly large when compared

to the ratios for He and the past calculations by Broad and Reinhardt [5] for H⁻, we find very good agreement between the time-dependent close-coupling and time-independent R-matrix methods over the entire energy range. The double ionization cross section is a smooth function of energy; the small structure found in the time-independent R-matrix method is due to pseudoresonances.

In summary we have applied the time-dependent close-coupling method to calculate various correlated photoionization processes in H⁻. The double to single photoionization cross-section ratios for H⁻ are almost twice as large as those found for He [1], but are in very good agreement with recent R-matrix method results [7]. We hope these theoretical predictions for H⁻ will serve to inspire future experimental measurements of correlated photoionization processes in this, the simplest of all negative atomic ions.

[1] M. S. Pindzola and F. Robicheaux, Phys. Rev. A **57**, 318 (1998).

[2] R. Wehlitz, I. A. Sellin, O. Hemmers, S. B. Whitfield, P. Glans, H. Wang, D. W. Lindle, B. Langer, N. Berrah, J. Viefhaus, and U. Becker, J. Phys. B **30**, L51 (1997).

[3] J. C. Levin, G. B. Armen, and I. A. Sellin, Phys. Rev. Lett. **76**, 1220 (1996).

[4] R. Dorner, T. Vogt, V. Mergel, H. Khemliche, S. Kravis, C. L. Cocke, J. Ullrich, M. Unverzagt, L. Spielberger, M. Damrau, O. Jagutzki, I. Ali, B. Weaver, K. Ullmann, C. C. Hsu, M.

Jung, E. P. Kanter, B. Sonntag, M. H. Prior, E. Rotenberg, J. Denlinger, T. Warwick, S. T. Manson, and H. Schmidt-Bocking, Phys. Rev. Lett. **76**, 2654 (1996).

[5] J. T. Broad and W. P. Reinhardt, Phys. Rev. A **14**, 2159 (1976).

[6] C. A. Nicolaides, C. Haritos, and T. Mercouris, Phys. Rev. A **55**, 2830 (1997).

[7] K. W. Meyer, C. H. Greene, and B. D. Esry, Phys. Rev. Lett. **78**, 4902 (1997).